13(2): 026-033 (2019)

Journal of FisheriesSciences.com

E-ISSN 1307-234X

Research Article

Research on Motion Response and Sickness Incidence of the Fishing Boat in Heading and Quartering Seas

Zhang Bao-Ji*, Ma Song-Nan

College of Ocean Science and Engineering, Shanghai Maritime University, Shanghai, China

Received: 15.05.2019 / Accepted: 03.06.2019 / Published online: 10.06.2019

Abstract: In order to reduce the surging acceleration of ocean fishing boats and improve the comfort of crews, based on the theory of regular wave and irregular wave potential flow, the six- Degree-of-Freedom (6DOF) motion performance, wave excitation forces and seasickness incidence of crew before and after modification of an ocean fishing boats were predicted and analyzed by panel method. The forecasting results show that the motion range of the modified fishing boats is obviously reduced and the seasickness incidence has been significantly improved.

Keywords: Motion response; Sickness incidence; Fishing boat; Heading and quartering seas

*Correspondence to: **Zhang Bao-Ji**, College of Ocean Science and Engineering, Shanghai Maritime University, Shanghai 201306, China, Tel: 86-13774353361; E-mail: zbj1979@163.com

Journal abbreviation: **J FisheriesSciences.com**

Introduction

When a fishing boat is sailing at high speed, its longitudinal overturning moment is bigger and its restoring moment is smaller, which results in a larger heave and pitch range of the hull and seriously affects its navigation performance. Moreover, the severe heave and pitch motion will also produce excessive longitudinal acceleration, which will cause seasickness and seriously reduce work efficiency. Therefore, reducing the longitudinal motion amplitude and seasickness rate of fishing boats has become a core issue in the design of fishing vessels. An important indicator of seaworthiness is Motion Sickness Incidence (MSI), which is the percentage of seasickness after two hours of voyage. MSI is less than 10% for passenger ships (Colwel, 1994).In order to improve the stability of longitudinal motion of fishing vessels and reduce the rate of seasickness, anti-rolling appendages must be installed. Among them, T-wing is widely used to improve the added mass and damping of ships as anti-rolling appendages, but as a longitudinal anti-rolling device, T-wing may increase navigation resistance. Therefore, it is necessary to combine with the wave plate to ensure that the resistance will not increase while the rolling is reduced. About the study of seasickness rate, O'Hanlan and McCawley (1973) used a mathematical expression to define the percentage of subjects who vomited within two hours after experimentation over 300 personnel under the name of MSI. Tezgodan's et al. (2014) studied operability index of ships using seakeeping analysis and performed such method on catamaran case study comparing to human comfort criteria. Liu (2018) studied the longitudinal motion of high-speed ferry controlled by T-wing; Liu (2018) studied the change of motion performance and seasickness rate of trimaran with or without T-wing; Zhang (2017) studied the longitudinal motion stability of catamaran controlled by T-wing. Tomasz (2012) discusses the influence of those environmental conditions on the human being that may cause motion sickness incidence. Santos (2015) with T-wing and wave plate as anti-rolling devices, the longitudinal motion amplitude of the hull can be reduced by 36% and the MSI amplitude by 45% for 40 speed high-speed boats under 5-class sea conditions. Nguyen (2015) studied the effects of roll motion on a MSI of a small boat and to access the comfort of passenger on board cruises based on wave energy spectrum. Seung-Jae et al. (2014) studied the improvement of MSI by ship hull form modification of the training ship. Youn-Kyoung (2012) analysed the MSI of the changing factors of the ship operational environment. From the above research, most scholars use T-wing for motion control, without considering the drag increase and wave drift caused by T-wing while improving its motion performance. Therefore, on the basis of summarizing the previous research results, taking a fishing boat as an example, based on the theory of regular wave and irregular wave potential flow, the panel method is used to install T-wing and its mother type respectively. The 6DOF Response Amplitude Operators (RAO) curves, wave drift force and seasickness rate before and after modification was compared. The results show that the motion amplitude of the ship with T-wing and flap is obviously improved, and the seasickness rate is obviously reduced. The research method in this paper can provide technical support for the improvement of the motion performance of the same ship.

Methodology

Potential flow theory

Panel method: To estimate the ship motion behavior, the coordinate fixed on the ship's Center of Gravity (CoG) shall be clarified first, which is called body-bound coordinate system G (xb,yb,zb).the ship motions are defined in the six degree of freedom around CoG. The translator displacements in the x, y, and z directions are respectively the surge, the sway, and the heave. The rotational displacements about the x, y, and z axes are respectively the roll, the pitch, and the yaw (Wang, 2016). The coordinate system and the linear and angular displacements are shown in Figure 1.

The total velocity potential can be expressed as:

$$\Phi = \varphi + \varphi_I \tag{1}$$

Where, ϕ is the perturbation potential, ϕ_I is the incident potential. The perturbed potential can be solved by Laplace equation

$$\nabla^2 \phi = 0 \tag{2}$$

In addition, the velocity potential should satisfy hull boundary condition and free surface boundary condition.

$$\frac{\partial^2 \phi}{\partial t^2} + g\frac{\partial \phi}{\partial z} = 0 \quad \text{On z=0} \tag{3}$$

Where t is the time, g is gravitational acceleration. The hull boundary condition is expressed as:

$$\frac{\partial \varphi}{\partial n} = V.n - \frac{\partial \varphi_I}{\partial n} = 0 \text{ On the hull surface} \tag{4}$$

Where n is the unit normal pointing into the fluid, V is the instantaneous velocity of the body.

In addition, the boundary condition in bottom is

$$\frac{\partial \phi}{\partial n} = 0, \; z \to -\infty \tag{5}$$

Radiation condition: $r = \sqrt{x^2 + y^2}$

$$\phi \to 0, r \to \pm\infty \tag{6}$$

Considering that there is no wave at infinity, moreover, the boundary value problem must satisfy the initial condition t=0

$$\varphi = 0 \text{ and } \frac{\partial \phi}{\partial t} = 0 \tag{7}$$

The velocity potential of the incident wave satisfied Laplace equation, it linearizes the boundary condition on the free surface and bottom. The velocity potential is solved by Equation (8):

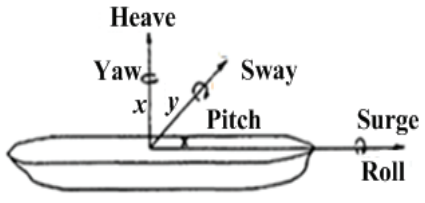

Figure 1: Definition of ship motion in 6DOF.

$$\varphi_I = \mathrm{Re}\left\{ \mathrm{i}\frac{ga}{\omega} e^{i(kx\cos\chi + ky\sin\chi)} e^{kz} e^{iwz} \right\} \quad (8)$$

Where, a is the amplitude, ω is the wave frequency and k is the wave number.

The hydrodynamic pressure at hull is given by Bernoulli's Equation:

$$p_T(P,t) = -\rho\left[\frac{\partial\phi}{\partial t} + \frac{1}{2}|\nabla\Phi|^2 + g \right] \quad (9)$$

The hydrodynamic force of the hull can be expressed as

$$\mathrm{F_i}(t) = \int_{S_B(t)} \mathrm{p_T}(P_0,t)\mathrm{n_0}\,\mathrm{dS}, \quad \mathrm{i} = 1,2,...,6 \quad (10)$$

Where n_{0i} is the component of generalized normal pointing into the body.

The boundary value problem can be solved by Green's theorem, and the unknown source strength can be obtained by integrating the whole wet surface with the surface source method. The basic equation is as follows:

$$\begin{aligned} &-\frac{1}{4\pi}\iint_{S_B(t)} \sigma(Q,t)\frac{\partial G^{(0)}(P,Q)}{\partial n}dS = -n.(V - \nabla\varphi_I()P,t))\frac{1}{n} \\ &+\frac{1}{4\pi}\int_0^t \left[\iint_{S_B(\tau)} \sigma(Q,t)\frac{\partial G^{(t)}(P,Q,t,\tau)}{\partial n}dS \right] d\tau \\ &-\frac{1}{4\pi} - \frac{1}{g}\int_0^t \left[\int_{\Gamma_F(\tau)} \sigma(Q,t)\frac{\partial G^{(t)}(P,Q,t,\tau)}{\partial n} u_n U_N d\Gamma \right] d\Gamma \end{aligned} \quad (11)$$

Where G is the Green's function, σ is the source strength, $P = P(x,y,z)$ is the field point, $Q = Q(x',y',z')$ is the source point.

$$\begin{aligned} &\varphi(P,t) = \frac{1}{4\pi}\iint_{S_B(t)} \sigma(Q,t)G^{(0)}(P,Q)dS \\ &+\frac{1}{4\pi}\int_0^t \left[\iint_{S_B(\tau)} \sigma(Q,t)G^{(t)}(P,Q,t,\tau)dS \right] d\tau \\ &-\frac{1}{4\pi} - \frac{1}{g}\int_0^t \left[\int_{\Gamma_F(\tau)} \sigma(Q,t)G^{(t)}(P,Q,t,\tau)u_n U_N d\Gamma \right] d\tau \end{aligned} \quad (12)$$

The time derivative of the disturbed velocity potential ϕ is expressed the following form approximately In Bernoulli's equation.

$$\frac{\partial\phi}{\partial t} \approx \frac{\phi_k - \phi_{k-1}}{\Delta t} - V.\nabla\phi \quad (13)$$

Where ϕ_k is the velocity potential of the time step k. The time derivative of the velocity potential is determined by solving boundary value problem.

$$\frac{\partial\varphi}{\partial t} = \frac{d}{dt}\left[(V - \nabla\varphi_I).n \right] \quad \text{on the hull surface} \quad (14)$$

The right side of the above equation can be further expanded to obtain the surface of the object velocity potential ϕ and boundary condition S_B

$$\frac{\partial\phi}{\partial n} = n.\left[(u + \omega + r) - (\omega \times u) \right] - n.\left[\frac{\partial\nabla\varphi_I}{\partial t} + ((u + \omega \times r).\nabla)\nabla\varphi_I - (\omega \times \nabla\varphi_I) \right] \quad (15)$$

Evaluation of excitation forces: The excitation forces were given as following (Garcia-Abril et al. 2017):

$$F_j = -\rho\iint_s n_j \left(i\omega_e - U\frac{\partial}{\partial x} \right)(\varphi_I + \varphi_D)ds \quad (16)$$

This expression can be separated into its incident wave part and diffraction part respectively as the following:

$$F_j^I = -\rho\iint_s n_j \left(i\omega_e - U\frac{\partial}{\partial x} \right)\varphi_I ds \quad (17)$$

$$m_0 = \int_0^\infty S(\omega)d\omega = \int_0^\infty S(\omega_e)d\omega_e \quad (18)$$

The encounter wave energy spectrum: In the study of the ship motions in waves, the frequency and the encountered frequency need to be converted. The encountered frequency depends on wave velocity, ship speed and wave propagation direction, as shown in Figure 2. Supposed that the ship is sailing in deep water, according to the relation of wave velocity in deep water, the encountered frequency can be converted as follows (Nielsen, 2017):

$$\omega_e = \omega - \frac{\omega^2 U}{g}\cos\mu \quad (19)$$

Where, U is the ship speed, g is the gravity acceleration, ω is the wave frequency, μ is the encountering angle, quartering seas wave condition at μ =135°, a heading wave condition at μ =180°.

For any reference systems, the total energy of waves is fixed. Therefore, the conversion of spectrum and encountered spectrum can be accomplished by the following formula:

$$m_0 = \int_0^\infty S(\omega)d\omega = \int_0^\infty S(\omega_e)d\omega_e \quad (20)$$

$$S(\omega_e)d\omega_e = S(\omega)d\omega \quad (21)$$

Also

$$\omega_e = \omega - \frac{\omega^2 U}{g}\cos\mu \quad (22)$$

$$\frac{d\omega_e}{d\omega} = 1 - \frac{2\omega U}{g}\cos\mu \quad (23)$$

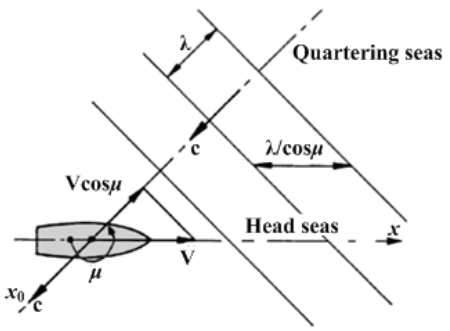

Figure 2: Encountering angle μ.

Therefore, the wave energy spectrum of the encountered frequency is:

$$S(\omega_e) = \frac{S(\omega)}{\left|1 - \frac{2\omega U}{g}\cos\mu\right|} \quad (24)$$

The ITTC dual parameter spectrum is selected as the wave model and the wave characteristic periods and significant wave height must to be input before the calculation. Figure 3 shows the density curve of wave spectrum with 3 meters significant wave height and 6.7 seconds characteristic periods. The dotted line is the ITTC dual parameter spectrum about the frequency, and the solid line is the density curve of wave spectrum about the encountered frequency at different ship speeds. It can be seen from the Figure 3, with the increasing of the speed, the position of the highest point reduces gradually, and the frequency value reaching the highest point increases gradually.

Motion analysis of the fishing boat with T-wing and flap

The fishing boat with T-wing and flap is shown in Figure 4. In this paper, the motion performance of fishing boats in regular and irregular waves before and after modification is simulated and compared in Table 1.

Motion analysis in regular wave: The sea conditions and

Table 1: Principal particulars of the ship.

Feature	Values	Feature	Values
Length between perpendiculars: L_{PP}	34.5 m	Mean draught: d_m	2.65m
Breadth: B	7.60 m	Block coefficient: C_B	0.597
Depth: D	3.07 m	Radius of gyration in pitch	0.36L_{OA}
Fore draught: d_f	2.50 m	Radius of gyration in heave	0.24 L_{OA}
Aft draught: d_a	2.80 m	Radius of gyration in roll	0.24 L_{OA}

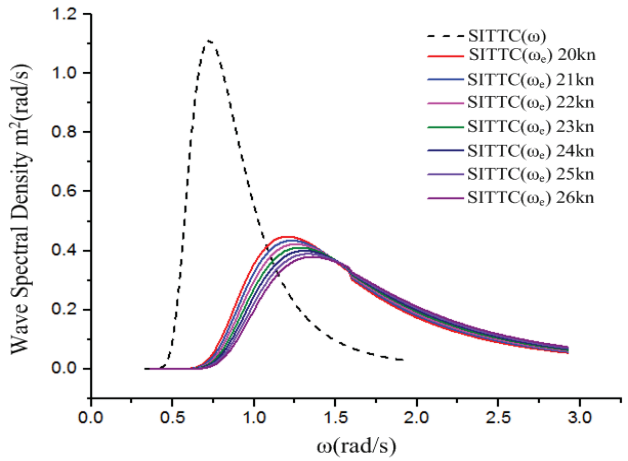

Figure 3: Curves of wave spectral density function at different speeds.

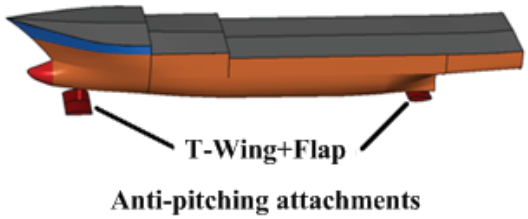

Figure 4: The model of the fishing boat with T-wing and flap.

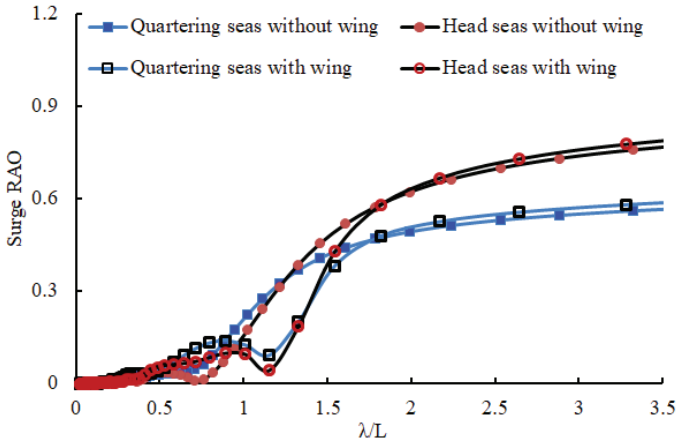

Figure 5: The surge RAO of the fishing boat.

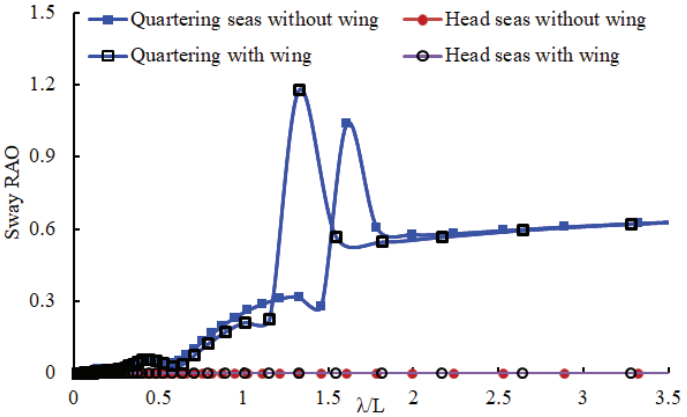

Figure 6: The sway RAO of the fishing boat.

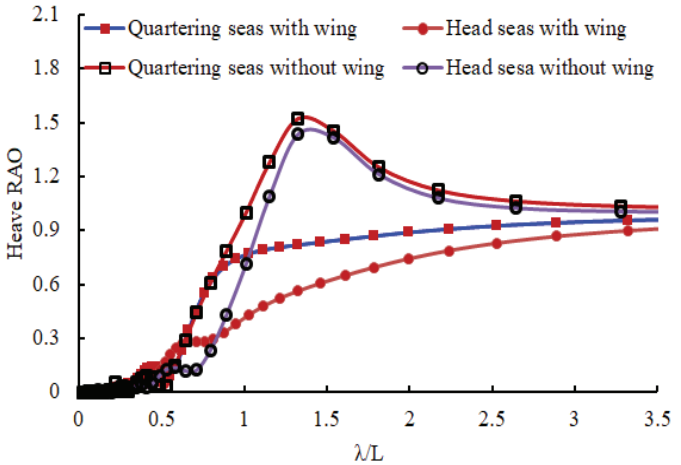

Figure 7: The heave RAO of the fishing boat.

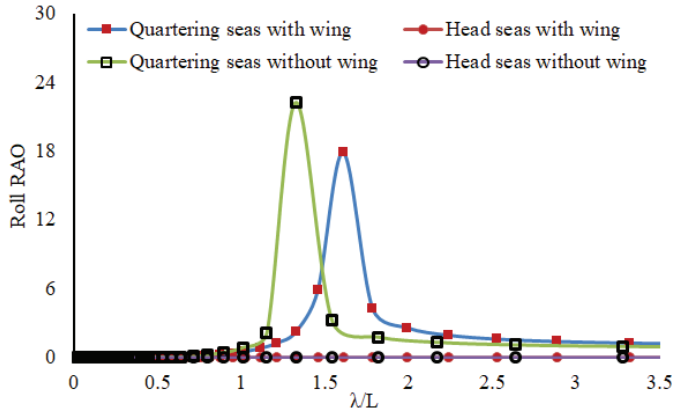

Figure 8: The roll RAO of the fishing boat.

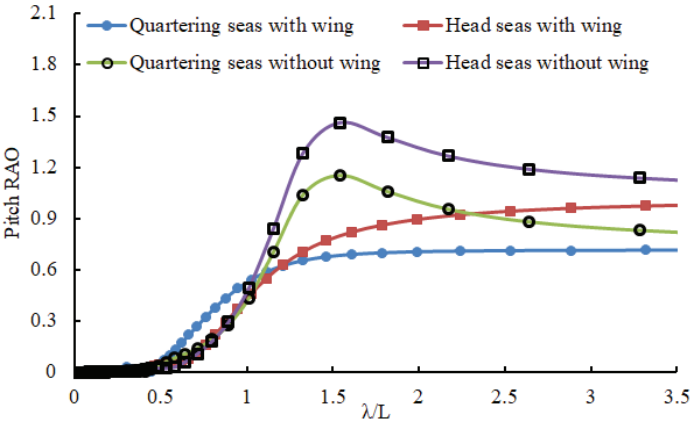

Figure 9: The pitch RAO of the fishing boat.

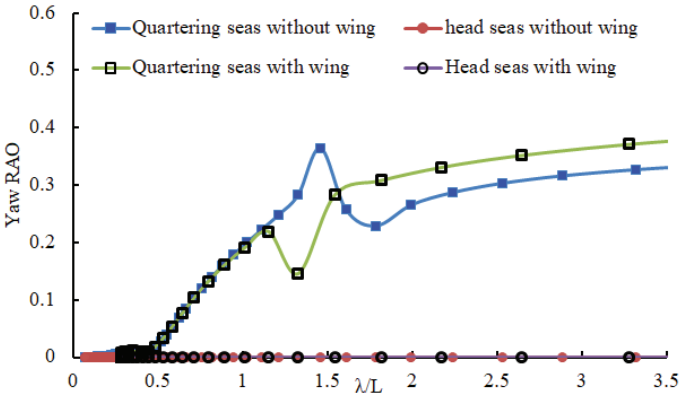

Figure 10: The yaw RAO of the fishing boat.

simulated wave conditions are shown in Table 2. The angle of wave direction is 180°of upstream wave and 135°of tail slant wave.

Figures 5-11 are motion response curve of fishing boat in regular wave; the figures shows that the 6-DOF (pitching, rolling, bowing, sagging, surging and swaying) and wave drag increase of fishing vessels with T-wing and flap are reduced to varying degrees compared with those before the modification.

Motion analysis in irregular wave: Figures 12 and 13 are the simulation results of fishing vessels in irregular waves before and after the installation of T-wing and flap. Here, only three degrees of freedom, heave/pitch and roll, which have the greatest impact on fishing vessels, are simulated, as can be seen from the figure. The degree of reduction of motion response of three degrees of freedom is also very obvious.

Wave excitation forces: Figures 14-16 show the computed wave exciting forces of the Surge, heave and yaw. It can be seen from the figure that the three kinds of wave induced forces are larger at low frequencies and smaller at high frequencies.

Table 2: Calculation condition of the regular wave.

Wave steepness H/λ	Wave height H(m)	λ/L	Wave length λ (m)	Average period T (s)
1/25	0.575	0.25	8.63	2.931
1/25	1.15	0.50	17.25	4.145
1/25	1.725	0.75	25.88	5.077
1/25	2.3	1.00	34.5	5.862
1/25	2.875	1.25	43.13	6.554
1/25	3.45	1.50	51.75	7.180
1/25	4.025	1.75	60.38	7.755
1/25	4.6	2.00	69.00	8.291

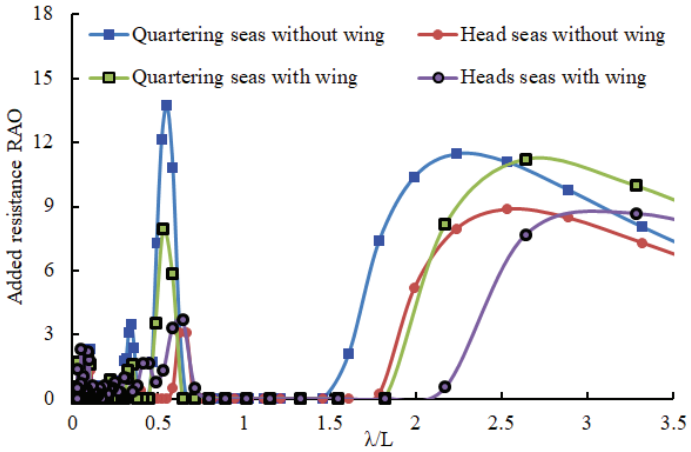

Figure 11: The added resistance RAO of the fishing boat.

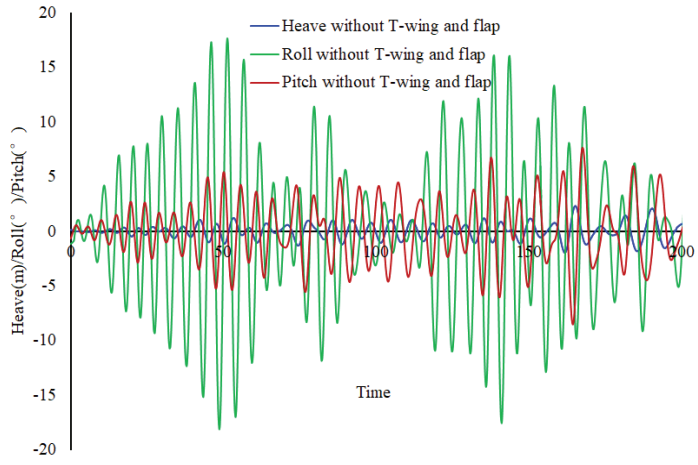

Figure 12: The fishing boat without T-wing and flap.

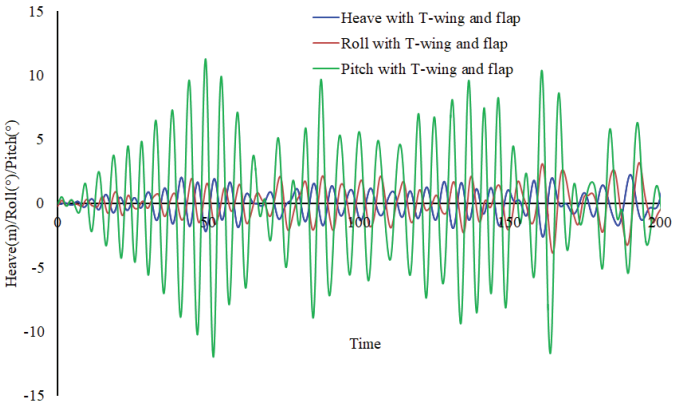

Figure 13: The fishing boat with T-wing and flap.

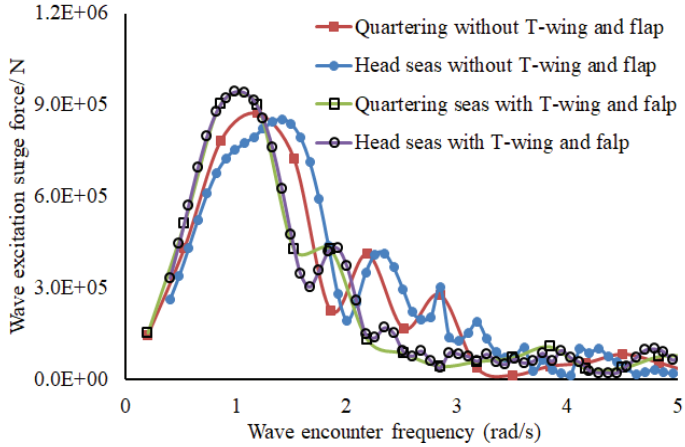

Figure 14: Wave excitation Surge force.

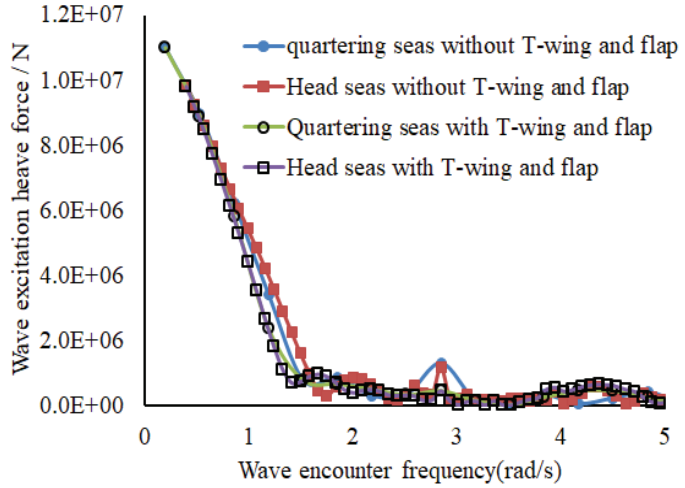

Figure 15: Wave excitation Heave force.

Moreover, the effect of T-wing and flap on wave induced forces is not significant. Therefore, the modified ship type will not lead to deterioration of its motion performance.

Calculation method of the MSI

Motion sickness is one of the important parameters that need to be investigated since they have a great effect on the crew's performance and also on passengers' comfort. MSI indicates the percentage of people experiencing vomiting when exposed to motion for a certain of time. The method uses a statistically-based, response surface which models the laboratory observations form two landmark parametric studies on motion induced sickness.

$$MSI(\omega_{ecentre}) = \int_{\omega_{e1}}^{\omega_{e2}} S_{vert-accel}(\omega_e) d\omega_e \quad (25)$$

MSI calculation formula by Lloyd: MSI after 2 hours exposure described as below expression:

$$MSI\% = 100 \times \Phi\left(\frac{\log_{10}(\frac{|\bar{S}_3|}{g}) - \mu_{MSI}}{0.4} \right) < 10\% \quad (26)$$

Where Φ(x) is the accumulation normal distribution function of the mean is 0 and the standard deviation is 1.μ_{MSI} is parameter calculated from this equation.

(1) μ_{MSI} calculation formula by Lloyd

$$\mu_{MSI} = 0.819 + 2.32(\log_{10} \omega_e)^2 \quad (27)$$

(2) μ_{MSI} calculation formula by O'Hanlon

$$\mu_{MSI} = 0.654 + 3.679(\log_{10} f_e) + 2.32(\log_{10} f_e)^2 \quad (28)$$

Where $\omega_e = 2\pi f_e$ $\omega_e = \sqrt{\frac{m_4}{m_2}}$, Vertical acceleration $\Phi(z) = \frac{1}{2\pi}\int_{-\infty}^{z} e^{\frac{1}{2}\chi^2} d\chi$

MSI calculation formula by Colwel: The initial exposure motion sickness incidence, MSI% is defined as follows. The subscript I is used to emphasize that this method is only used during the initial exposure phase (Nguyen and Hien, 2015)

$$MSI\% = 100 \times \Phi(Z_a)\Phi(Z_t') \quad (29)$$

Where, Φ is the cumulative distribution function of the standardized normal variable z

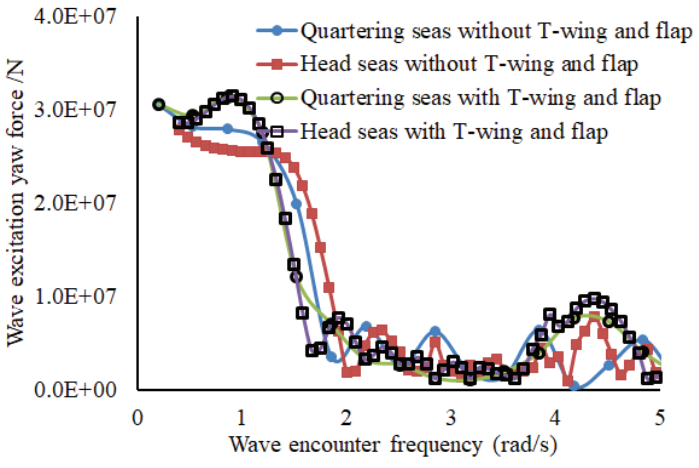

Figure 16: Wave excitation Yaw force.

$$\Phi(z)=\frac{1}{2\pi}\int_{-\infty}^{z}e^{\frac{1}{2}\chi^2}d\chi \tag{30}$$

The standardized normal variables z_a and z'_t are defined as follows,

$$z_a=\frac{\log_{10}a-\mu_a(f)}{\sigma_a} \tag{31}$$

$$z_t^{'}=\frac{Z_t-\rho z_a}{\sqrt{1-\rho^2}},\quad z_t=\frac{\log_{10}t-\mu_t}{\sigma_t}$$

Where a is the Root Mean Square (RMS) vertical acceleration (g); f is the modal frequency (HZ) of a, and t is the duration of exposure (min).

$$\mu_a=0.87+4.36(\log_{10}f)+2.73(\log_{10}^2 f) \tag{32}$$

Where,

μ_t=1.46, σ_a=0.47, σ_t=0.76, ρ=-0.75

After manipulation, this method reduces to the following equations.

$$\mathrm{MSI}\%=100\times\Phi(Z_a)\Phi(Z_t^{'}) \tag{33}$$

Where

$$z_a=2.128(\log_{10}a)-9.277(\log_{10}f_e)-5.809(\log_{10}f_e)^2-1.851$$

$$z_t^{'}=1.134z_a+1.989(\log_{10}t)-2.904$$

MSI% calculation of the fishing boats: The calculated wave conditions in this paper are shown in Table 3, the vertical acceleration is shown in Figure 17, and the MSI% of deck and cabin is compared as shown in Figures 18 and 19.

Table 3: Wave description, heights and average periods.

Wave Description	Characteristic Height (m)	Average period (s)
Moderate	0.575	2.931
Rough	1.725	6.571
Very rough	3.45	7.18

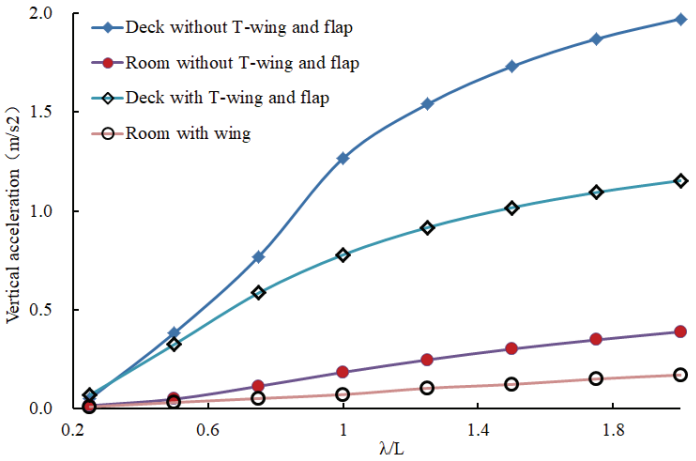

Figure 17: Graphic of vertical acceleration *vs.* Wavelength/ Length.

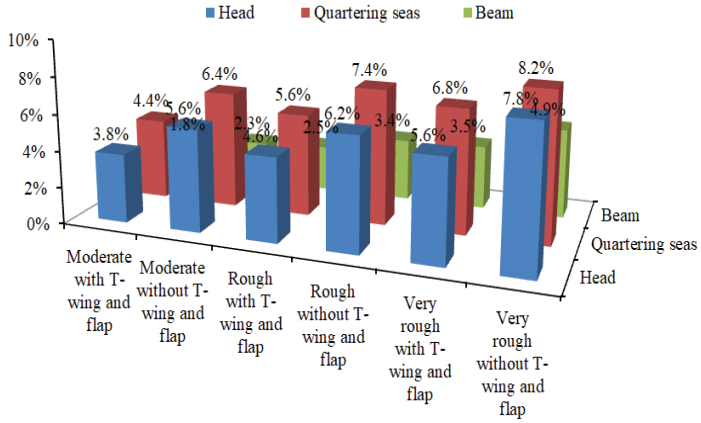

Figure 18: Deck MSI % difference.

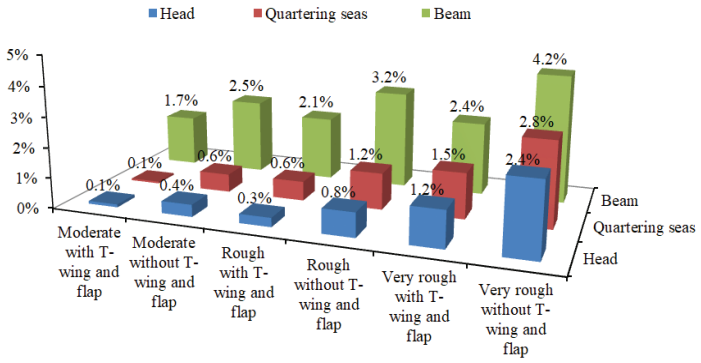

Figure 19: Room MSI% Difference.

The vertical acceleration of the ship is one of the important parameters to be noticed when considering the behavior of ships considering Motion Sickness; other acceleration components seem to have minor effects on MSI. From the data given by the Panel Method program, values are taken for phases and amplitudes in heave and pitch with which calculation is made of accelerations for each point and these are seen in Figure 17, it may be noted that the highest accelerations occur in the deck; these are given for wavelength/ship ratios between 2.0. The lowest accelerations occur in the room.

The MSI % has been indicated in Figures 18 and 19.It can be seen from the figure that the MSI% on deck is the largest in tail inclined wave and the MSI% in cabin is the largest in transverse wave. Moreover, the MSI% of deck and cabin decreases obviously under the action of three levels of wave.

Conclusion

Based on the theory of regular wave and irregular wave potential flow, the 6DOF motion response, induced wave force and seasickness rate of fishing vessels before and after modification were calculated by panel method. The results show that the 6DOF motion amplitude of fishing vessels with T-wing and flap devices has been reduced, seasickness rate has been improved obviously, and induced wave force has not changed much.

Using Panel method to calculate the motion response and sickness incidence of the fishing ship will have a certain gap with the experimental value. The calculation result of CFD method

will be more accurate, which will be the next research plan of this paper.

Acknowledgments

This research was supported by the National Natural Science Foundation of China (No. 51779135, 51009087), Shanghai Natural Science Foundation of China (No. 14ZR1419500).

References

Colwell, J.L. (1994) Motion sickness habituation in the naval environment.

O'Hanlon, J.F., McCauley, M.E. (1973) Motion sickness incidence as a function of the frequency and acceleration of vertical sinusoidal motion, DTIC Document.

Tezdogan, T., Incecik, A., Turan, O. (2014) Operability assessment of high speed passenger ships based on human comfort criteria. Ocean Engineering 89, 32-52.

Liu, Y.W., Zheng, F.J., Qi Zhi, G. (2018) Control of longitudinal motion for high speed ferry. Electric Machines and Control 22(1), 114-120.

Liu, Z.L., Zheng, L.H., Zhang, W. (2018) Predictive Control for Longitudinal Motion of Trimaran with T-foil. Proceedings of the 37th Chinese Control Conference, Wuhan, China. pp: 25-27

Zhang, S.T., Sun, M.X., Liang L.H., Jiang, J.L. (2014) A controller design using state- feedback H∞ algorithm for T-foil of WPC. Ship Science and Technology 36(10), 78-82.

Tomasz, C. (2012) The prediction of the Motion Sickness Incidence index at the initial design stage. Scientific Publisher of the Maritime University of Szczecin 31(103), 45–48.

Santos, M., Lopez, R., de la Cruz, J.M. (2015) Fuzzy control of the vertical acceleration of fast ferries. Con Eng Prac 13, 305-313.

Nguyen, A.T., Hien, L.T. (2015) Study of the effects of roll motion on transverse stability of a small boat. International Journal of Mechanical Engineering and Applications 3(1-3), 24-28.

Han, S.J., Lee, S.C., Ha, Y.R. (2014) A Study on the Improvement of MSI by Ship Hull Form Modification of the Training Ship. Journal of Fisheries and Marine Science Education 26(4), 686-694.

Han, S.J., Lee, S.C., Ha, Y.R. (2014) A Study on the Motion Sickness Incidence due to Sea State and Location of the Training Ship Kaya. Journal of Fisheries and Marine Science Education 26(1), 126-133.

Ku Youn, K. (2012) Analysis for Motion Sickness Incidence (MSI) of the Changing Factors of the Ship Operational Environment. Master's Thesis, Mokpo National Maritime University of Graduate School, South Korea.

Wang, J. (2016) Time-Domain Simulation of Wave-Induced Ship Motions by a Rankine Panel Method. Master's thesis, Memorial University of New foundland, Canada.

Garcia-Abril, M., Paparella, F., Ringwood, J.V. (2017) Excitation force estimation and forecasting for wave energy applications. IFAC Papers Online 50(1), 14692–14697.

Nielsen, U.D. (2017) Transformation of a wave energy spectrum from encounter to absolute domain when observing from an advancing ship. Appl Ocean Res 69, 160-172.

Nguyen, A.T., Hien, L.T. (2015) Study of motion sickness incidence in ship motion. Sci Tech Dev J 18(4), 102-109.